Journal of Biomechanics 44 (2011) 424–429

Contents lists available at ScienceDirect

Journal of Biomechanics

journal homepage: www.elsevier.com/locate/jbiomech
www.JBiomech.com

Ultrasound echo is related to stress and strain in tendon

Sarah Duenwald [a], Hirohito Kobayashi [b], Kayt Frisch [a], Roderic Lakes [a,c], Ray Vanderby Jr.[a,b,*]

[a] Department of Biomedical Engineering, University of Wisconsin—Madison, 1550 Engineering Drive, Madison, WI 53706, USA
[b] Department of Orthopedics, University of Wisconsin—Madison, 600 Highland Avenue, Madison, WI 53792, USA
[c] Department of Engineering Physics, University of Wisconsin—Madison, 1500 Engineering Drive, Madison, WI 53706, USA

ARTICLE INFO

Article history:
Accepted 30 September 2010

Keywords:
Tendon
Ultrasound
Echo intensity
Acoustoelasticity

ABSTRACT

The mechanical behavior of tendons has been well studied *in vitro*. A noninvasive method to acquire mechanical data would be highly beneficial. Elastography has been a promising method of gathering *in vivo* tissue mechanical behavior, but it has inherent limitations. This study presents acoustoelasticity as an alternative ultrasound-based method of measuring tendon stress and strain by reporting a relationship between ultrasonic echo intensity (B-mode ultrasound image brightness) and mechanical behavior of tendon *in vitro*. Porcine digital flexor tendons were cyclically loaded in a mechanical testing system while an ultrasonic echo response was recorded. We report that echo intensity closely follows the applied cyclic strain pattern in time with higher strain protocols resulting in larger echo intensity changes. We also report that echo intensity is related nonlinearly to stress and nearly linearly to strain. This indicates that ultrasonic echo intensity is related to the mechanical behavior in a loaded tissue by an acoustoelastic response, as previously described in homogeneous, nearly incompressible materials.

Acoustoelasticity is therefore able to relate strain-dependent stiffness and stress to the reflected echo, even in the processed B-mode signals reflected from viscoelastic and inhomogeneous material such as tendon, and is a promising metric to acquire *in vivo* mechanical data noninvasively.

1. Introduction

Tendons translate muscular contraction into skeletal movement, storing and releasing energy during motion (Ker et al., 1987). Understanding tendon mechanics is therefore essential to understand normal and pathologic movement and for analyzing the structural and mechanical consequence of injury. Thus far, tendon mechanical data have been obtained largely through *in vitro* experimentation (Abrahams, 1967; Cohen et al., 1976; Ker, 2007; Rigby et al., 1959; Woo et al., 1982). Though such studies provide essential basic mechanical information about the tissue, a noninvasive method to acquire mechanical data would allow patient-specific analysis and direct analysis of human pathologies that are poorly modeled by animals (e.g., rotator cuff). *In vivo* tendon loads have been computed using force plates or dynamometers and geometrical information (Maganaris and Paul, 1999, 2000; Riemersma et al., 1988) and/or with EMG studies of muscle (Lloyd and Besier, 2003). Direct studies of tendon are typically invasive and often rely on implanted strain gauges, providing only local measure of strain and a partial measure of mechanical behavior. EMG estimates contractile force in muscle (and thus in tendon), but it has a number of limiting factors such as cross talk from different muscles, passive tissue effects, different muscle lengths during contraction, and dynamic motion.

Recently, ultrasound imaging has been used to evaluate tissue strain and other mechanical properties (Samani et al., 2007; Skovorada et al., 1994, 1995). Many researchers have tried to evaluate tissue strain and mechanical properties using elastography, a technique originally proposed by Ophir et al. (1991), which maps strain distributions in tissues resulting from compression on the surface; since strain is inversely related to stiffness, elastography is an indirect method to estimate tissue stiffness (Doyley et al., 2000; Kallel et al., 1996; Kallel and Bertrand, 1996; Ponnekanti et al., 1992, 1995). Though researchers have used this technique to identify tissue properties, current elastographic methods have some inherent limitations.

Elastography tracks inhomogeneous echo reflections ("speckles" resulting from tissue heterogeneities) in ultrasound images during loading (usually using the transducer to apply compression); strain information calculated using distortions of these reflectors is related to mechanical properties via post hoc mechanical analysis. A limitation of elastography is that it is inherently linear, assuming that the material properties as well as ultrasound wave velocity do not change during strain measurement, which restricts analyses to small increments of compression. When soft tissues were tested under larger deformations and were therefore nonlinear in stiffness, significant errors occurred (Itoh et al., 2006; Zhi et al., 2007). This is problematic in soft tissues such as tendons

* Correspondence to: Room 5059, 1111 Highland Avenue, Madison, WI 53705, USA. Tel.: +1 608 263 9593; fax: +1 608 265 9144.
E-mail address: vanderby@ortho.wisc.edu (R. Vanderby Jr.).

0021-9290/$ - see front matter © 2010 Elsevier Ltd. All rights reserved.
doi:10.1016/j.jbiomech.2010.09.033

as they are nonlinear in stiffness and undergo relatively large deformations during activity, reaching strains of several percent (elastography works best when strain increments are restricted to less than 1%). Another limitation is the commonly used method of compressive testing; tendon is loaded in tension *in vivo*, so interesting mechanical information is lost when only considering compressive transverse loads. These restrictions associated with standard elastographic methods limit its applicability to tendon. Finally, elastography measures strain. More data are needed, either stress or stiffness, to completely describe the mechanical behavior.

The theory of acoustoelasticity, developed byHughes and Kelly (1953) is based on the principle that the acoustic properties of a material are altered as the material is deformed and loaded, similar to a change in tension alters the pitch of a guitar string. Changes in acoustic properties caused by elastic deformation can be measured as a change in wave propagation velocity or reflected wave amplitude (Kobayashi and Vanderby, 2005, 2007). Kobayashi and Vanderby (2005, 2007) derived the acoustoelastic relationship between reflected wave amplitude and mechanical behavior (strain-dependent stiffness and stress) in a deformed, nearly incompressible material using A-mode 1-D ultrasound. Despite signal processing, this phenomenon is also manifested in B-mode 2-D ultrasound, as the tensioning of tendon increases the intensity of the reflected ultrasonic echoes, leading to a brighter ultrasound image in B-mode. Examples of this acoustoelastic effect in soft tissues have been reported in the literature. For example, mean echogenicity has been correlated to the elastic modulus of the equine superficial digital flexor tendon (Crevier-Denoix et al., 2005), and softening of the human extensor tendons has been detected with sonoelastography (De Zordo et al., 2009). Pan et al. (1998) reported increasing echo intensity when skin underwent increase in strain (13–53%). The present study examines the relationship between ultrasonic echo intensity from standard clinical B-mode images and the stress–strain behavior of tendon during controlled loading *in vitro*. Its purpose is to examine whether this acoustoelastic phenomenon has the potential for the functional evaluation of tendon *in vivo*.

2. Materials and methods

2.1. Specimen preparation

Eight porcine digital flexor tendons were carefully extracted from porcine legs (aged six months, sacrificed for an unrelated study) for *ex vivo* testing, leaving the bone and insertion site intact at the distal end. Bony ends were embedded in lightweight filler (Evercoat, Cincinnati, OH, USA) for ease of gripping. Specimens were kept hydrated in physiologic buffered saline (PBS) solution throughout preparation.

2.2. Mechanical testing

Mechanical testing was performed using a servohydraulic mechanical test system (Bionix 858; MTS, Minneapolis, MN, USA) with the custom bath shown in Fig. 1. The bony end of the tendon was secured in the metal block, attached to the bath, while the soft tissue end was secured in a moving grip, attached to the load cell. Grip-to-grip displacement was controlled by the servohydraulic system, and load was measured via a 50 lb load cell (Eaton Corporation, Cleveland, OH, USA). Once secured in the system, tendons were preloaded to 1 N to remove slack. Following preloading, tendons were preconditioned in a sinusoidal wave to 2% strain for 20 s and allowed to rest for 1000 s. Tendons were then subjected to cyclic mechanical testing to 2%, 4%, or 6% strain for 10 cycles at 0.5 Hz and allowed to rest for 1000 s to ensure complete recovery occurred between tests. The process was repeated until each specimen was tested at each of the three strain levels two separate times (in random order), for a total of six tests per tendon. To avoid strain history transient effects, the last three cycles were used for analysis (see Fig. 2) as tendon loads had effectively reached steady state.

2.3. Ultrasound

Cine ultrasound was recorded using a GE LOGIQ*e* ultrasound machine with GE 12L-RS Linear Array Transducer (General Electric, Fairfield, CT, USA). The ultrasound transducer (operating at 12 MHz) was held in fixed position in the custom bath (see Fig. 1) using a custom-built clamp fixed to the side of the bath to record cine B-mode ultrasound (20 frames per second) of the tendon during the mechanical testing outlined in the previous section. To avoid strain history transient effects and to correspond to the mechanical data, only the last three cycles were used for analysis. The overall echo intensity (i.e., the average gray scale brightness in a selected region of interest in a B-mode image) of the tendon, averaged over the entire region of interest (ROI) between the grips, was calculated for each frame in order to record the echo intensity changes over time.

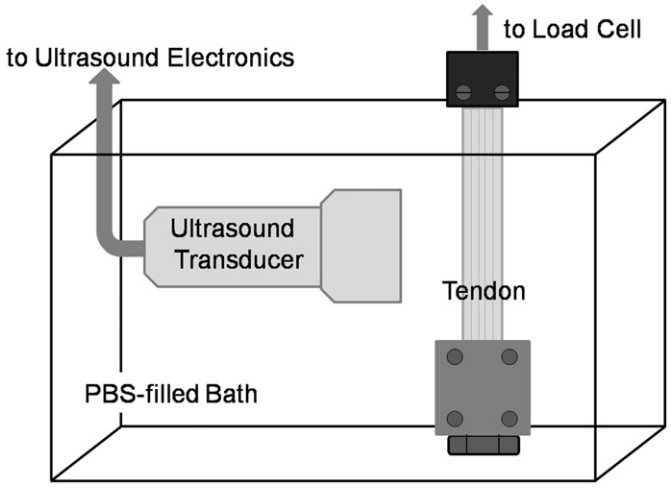

Fig. 1. Test setup. The tendon is held in place by a stationary metal block and a moveable soft tissue grip, which is connected to the load cell. The ultrasound transducer is submerged in the PBS bath and held in place to image the tendon during mechanical testing.

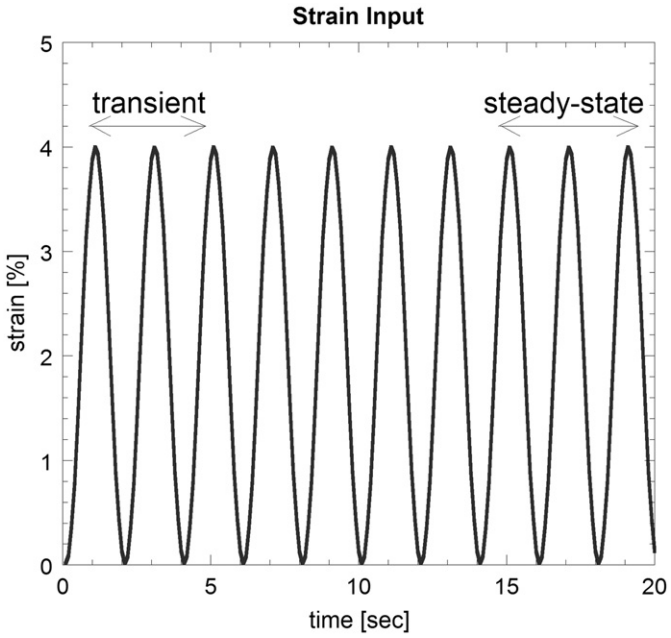

Fig. 2. Strain input for mechanical testing, shown for the 4% strain test. The first three cycles give rise to history dependent transient effects. Tissue has generally reached steady-state by the final three cycles. Data from the final three cycles are used in this study.

2.4. Region of interest tracking

In order to measure echo intensity changes over the ROI for the entire test, a region-based optical flow matching technique (Anandan, 1989; Barron et al., 1994) was used to track the movement of "speckles" (patterned echo reflections caused by tissue heterogeneity) in the ultrasonic echo that defined the ROI. This algorithm evaluated the speckle displacement between consecutive image frames by finding

the best-matching optical flow of elements that surrounded the selected speckles. It has been reported that the region-based optical flow matching technique that uses summed-square differences or cross-correlation coefficients as a metric is less sensitive to noise and fast motion (Anandan, 1989). This method was also used to track ultrasound speckles in three dimensional ultrasound images by Duan et al. (2009). In this study, we adopted a summed-squared difference metric based on region-based optical flow tracking to estimate the movement of speckles defining the ROI between two consecutive frames of cine (dynamic) ultrasound.

2.5. Repeatability

In order to determine the repeatability of the ultrasonic echo intensity on the same specimen, a single specimen was subjected to cyclic loading to 4% strain three times, and the ultrasound echo analysis was performed on the cine ultrasound images (captured during loading) three times, for a total of nine analyses of the specimen.

2.6. Predictions

Two types of predictions were compared. First, the relationship between echo intensity and strain recorded by the MTS was examined using data from the eight specimens undergoing mechanical testing, and the ability of an echo-based prediction (ε_{echo}) to calculate strain was compared to the ability of a curve fit of the mechanical test data (ε_{MTS}) to calculate strain. The root mean squared error (RMSE) between the ε_{echo} prediction and the data points, as well as between the ε_{MTS} curve fit and the data points, was calculated and compared.

Second, the relationship between echo intensity and stress, and the relationship between strain and stress were calculated using curve fits of the data from the mechanical testing, and the ability of an echo-based prediction to calculate stress was compared to the ability of a strain-based prediction to calculate stress. Predictions were also used to calculate stress in the repeatability specimen. The RMSE between predictions and the data points was calculated and compared. Stress predictions were then applied to the results from the repeatability study for further validation.

2.7. Statistics

To compare echo intensity changes at different strain levels, repeated measures ANOVA was used. Echo intensity change was compared between 2%, 4%, and 6% strains.

In order to analyze the repeatability testing, the average of all nine specimens was taken, and the variation of each analysis from the average was measured using the RMSE calculation. The RMSE values were then averaged, and this average was compared to zero using a *t*-test. Similar tests were done while determining the ability of predicting stress with strain and echo intensity, but the RMSE values were compared to each other rather than to zero.

3. Results

3.1. Mechanical testing

When subjected to the cyclic loading protocol as shown in Fig. 2, the ultrasonic echo intensity of tendon was cyclic in behavior, and the echo intensity change increased with increase in strain level, shown in Fig. 3. This figure also shows a nonlinear dependence of peak echo intensity versus strain amplitude, and a deviation in the 6% strain curve from sinusoidal shape. Consequently, the relationship between echo intensity and strain is more nonlinear in this range than at lower strains. The average changes in echo intensity during cycles to 2%, 4%, and 6% strains were $3.96 \pm 0.58\%$, $12.46 \pm 0.97\%$, and $24.45 \pm 2.21\%$, respectively. Echo intensity changes were significantly different at each strain level ($p < 0.0001$). Fig. 4 shows these averages along with the average load reached during the same cycles to 2%, 4%, and 6% strains.

Fig. 5a shows the stress–echo intensity and stress–strain relationship of a single specimen during a test to 4% strain, demonstrating the similarity of curve shape. The trend of nonlinearity between stress and strain as well as stress and echo intensity was consistent for all eight specimens (Fig. 5b). The shape of the echo intensity change correlated well with strain (more so than with stress).

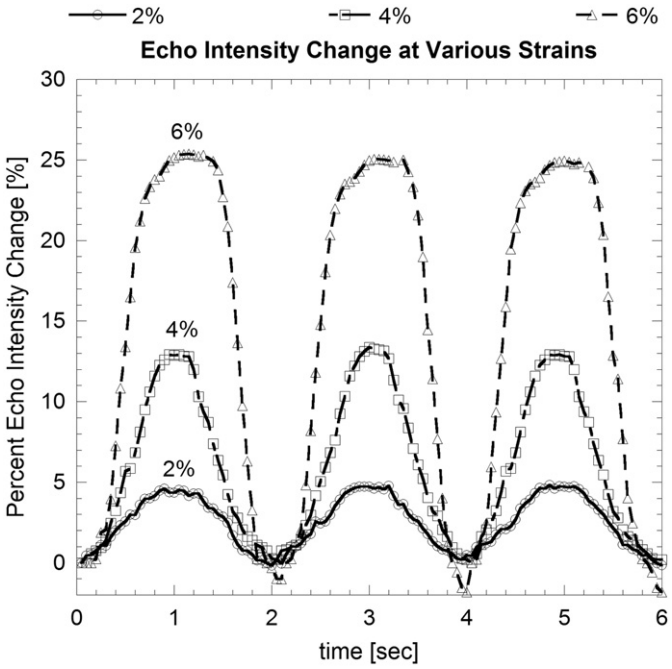

Fig. 3. Echo intensity change during cyclic loading to 2%, 4%, and 6% strain for a single specimen. Echo intensity follows a cyclic pattern for all three strain levels, and the increase in echo intensity depends on strain (greater for higher strains).

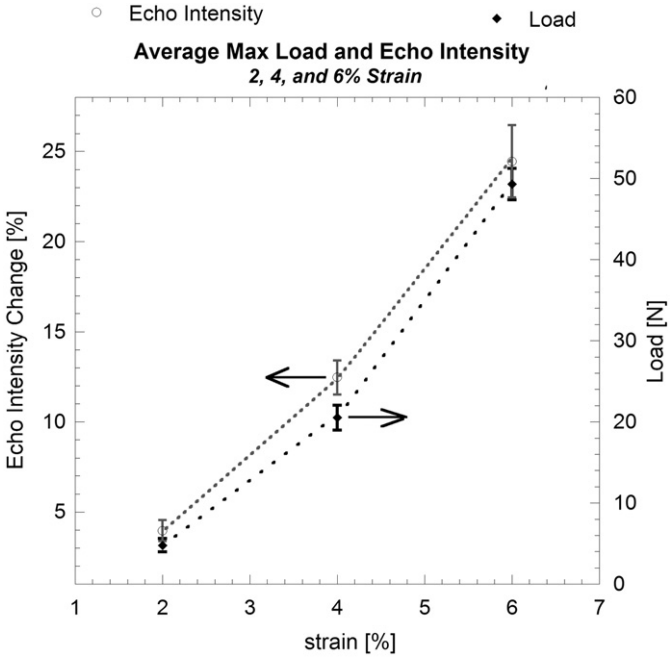

Fig. 4. Average change in echo intensity (percent) and average load reached during cycles to 2%, 4%, and 6% strains for eight specimens. Bars indicate one standard deviation from the mean. Arrows indicate the corresponding axes. Both mean load reached and mean echo intensity change during cyclic loading increases with strain.

3.2. Repeatability

Fig. 6 shows the echo intensity results of repeatability testing. Curves from all nine tests had the same shape and a maximum change in echo intensity of roughly 11% during testing to 4% strain. The deviation of each curve from the mean was calculated using a root mean squared error (RMSE); the RMSE averaged over all nine trials for the curve shown in Fig. 6 was $0.349 \pm 0.202\%$.

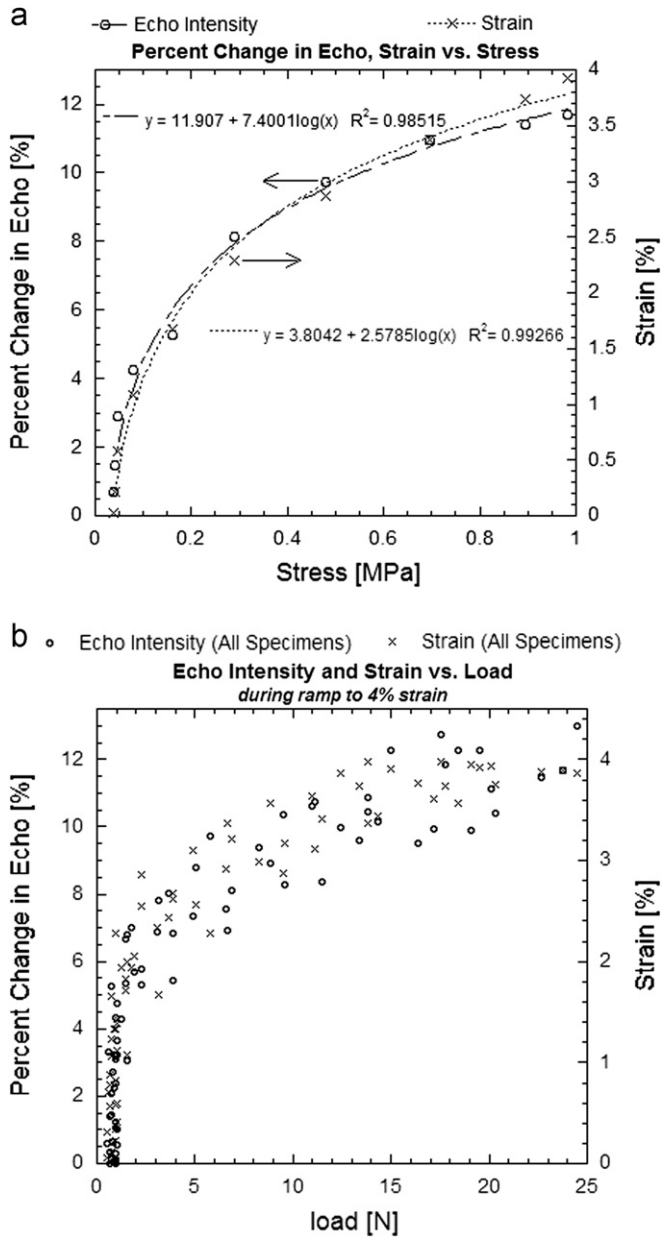

Fig. 5. Echo intensity change and strain versus stress during one half-cycle to 4% strain (stretch from 0% to 4%) for (a) one specimen (with logarithmic curve fits) and (b) all eight specimens. Open circles represent ultrasonic echo intensity data points and × 's represent strain data from the MTS test frame; arrows point to the corresponding axes. The stress–echo intensity relationship follows a similar shape as the stress–strain relationship.

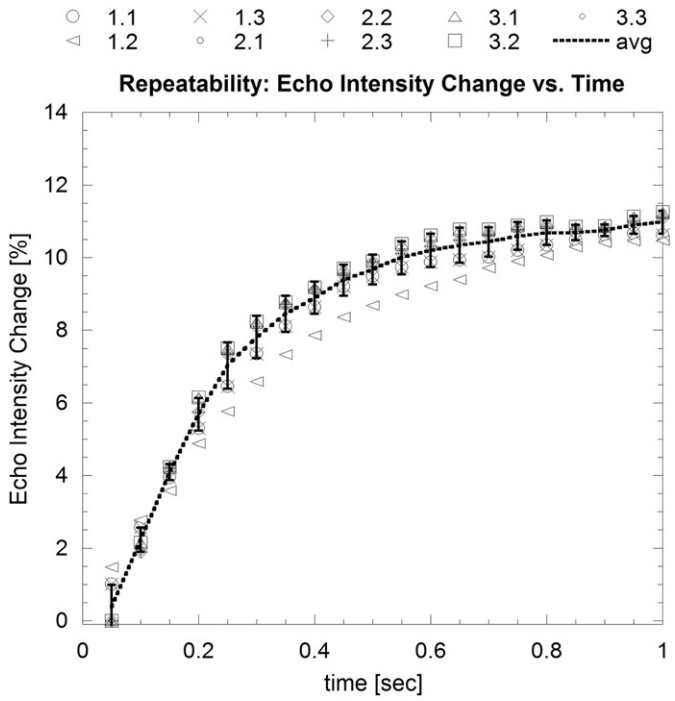

Fig. 6. Echo intensity change versus time during one half-cycle of repeatability testing (in the same fashion as the results in Fig. 2) to 4% strain. One specimen was subjected to three cyclic loading tests, and the echo intensity of each loading test was analyzed three times, for a total of nine echo intensity analyses. Trial numbers and corresponding symbols are labeled on the top of the graph. The dotted black line indicates the average of all nine analyses; black bars indicate one standard deviation.

3.3. Predictions

The echo data from the eight specimens in Fig. 5b was fitted with a logarithmic curve (Fig. 7a), which had the highest R^2 value of attempted fits. As the relationship between echo intensity change and strain was nearly linear, and the scale of the maximum echo intensity reached during the cycle to 4% strain was roughly three times the maximum strain, the following the linear relationship was used

$$\varepsilon_{\text{echo}} = \tfrac{1}{3}\text{echo} \tag{1}$$

where echo refers to the echo intensity change and $\varepsilon_{\text{echo}}$ refers to echo intensity-based prediction of strain. With the logarithmic fit for echo as a function of stress substituted in, this equation becomes

$$\varepsilon_{\text{echo}} = 3.7 + 2.29\log(\sigma) \tag{2}$$

where σ refers to stress. When used to fit the experimental strain data, this fit had an R^2 value of 0.871, compared to the R^2 value of 0.892 of the curve fit [$\varepsilon_{\text{MTS}} = 3.85 + 2.23\log(\sigma)$] of the strain data in Fig. 7b, where ε_{MTS} refers to strain data reported from a mechanical testing system. The average RMSE between the echo-based prediction ($\varepsilon_{\text{echo}}$) and the strain data points was 0.448 ± 0.169, and the average RMSE between the curve fit of the strain data from the MTS (ε_{MTS}) and the strain data points was 0.438 ± 0.136; these values were not significantly different ($p = 0.4513$), indicating that the echo-based prediction $\varepsilon_{\text{echo}}$ (based on the linear relationship echo$= 3\varepsilon$) was capable of predicting strain values at least as well as the curve fit of the strain data, ε_{MTS}, from the MTS.

Stress predictions were then calculated using the curve fits of the strain and echo data resulting in

$$\sigma_{\varepsilon} = 10^{(\varepsilon - 3.85/2.23)} \tag{3}$$

and

$$\sigma_{\text{echo}} = 10^{(\text{echo} - 11.07/6.89)} \tag{4}$$

Using these equations, stress was calculated as a function of strain (Eq. (3)) and as a function of echo intensity (Eq. (4)). Calculated stress values were compared to the stress data in Fig. 5b, and the RMSE between them calculated. The average RMSE for the stress calculated as a function of echo (σ_{echo}) was 0.17 ± 0.08 and for stress calculated as a function of strain (σ_{ε}) was 0.13 ± 0.07. These values were not significantly different ($p = 0.178$), indicating that echo intensity is able to predict stress as well as a direct measurement of strain, based on the experimental stress data.

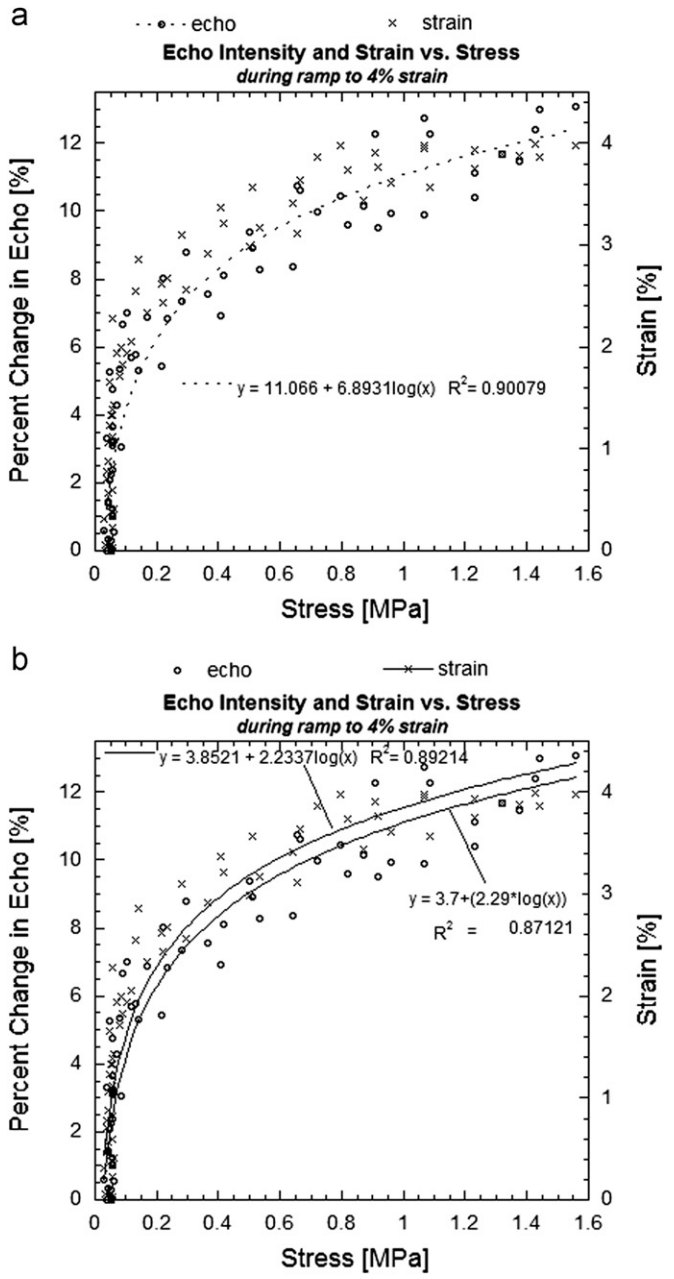

Fig. 7. Echo intensity and strain changes versus stress during one half-cycle (same data as in Fig. 4b) plotted with (a) logarithmic curve fit of echo intensity data [echo= 11.066+6.893 log(stress)] and (b) logarithmic curve fit of strain [strain=3.8521+ 2.2337 log(stress)] (top) and the linear echo-based approximation [strain=3.7+ 2.29 log(stress), or 1/3*(echo percent change)] (bottom). The linear approximation fits the experimental strain data nearly as well as the curve fit of the strain data, with no significant difference in RMSE. Open circles represent ultrasonic echo intensity data points and × 's represent strain data from the MTS test frame; arrows point to the corresponding axes.

When applied to data from the repeatability testing study, the RMSE for stress calculated as a function of echo (σ_{echo}) was 0.103 ± 0.016, and the RMSE for stress calculated as a function of strain (σ_{ε}) was 0.386 ± 0.001. Again, echo intensity was able to predict stress as well as directly measured strain. In fact, for this case the RMSE values for stress calculated from echo intensity were significantly lower ($p < 0.01$) than those for stress calculated from strain, indicating that for this set of experimental data echo intensity is more accurate than measured strain at predicting stress values.

4. Discussion

In this study, cyclic loading experiments were carried out on excised porcine digital flexor tendons in a mechanical testing system. Cine ultrasound images were simultaneously recorded in B-mode in order to compare ultrasonic echo intensity changes (i.e., the average gray scale brightness in a selected region of interest in each image) to directly measured stress and strain. We show, for the first time, that an acoustoelastic effect known to exist in homogeneous materials can be easily observed and related to stress and strain in tendon. The shape of the resulting echo intensity curve correlates well with strain, in a nearly linear relationship. The echo intensity behavior in time nearly perfectly follows the strain behavior in time, with only slight deviations during the cyclic loading to 6% strain level. Echo intensity, however, has a very nonlinear relationship with stress. While the plot of the peak echo intensity reached during cycles versus time closely resembles the plot of the peak load reached versus time, the echo intensity versus stress curve is highly nonlinear; the shape of this curve closely resembles the nonlinear stress versus strain curve. This suggests a relationship between echo intensity and geometrical change in the fibrous structure of the tissue as it is extended.

It should be noted that the relationships reported here, that correlate stress and strain to B-mode echo intensity, are for this well-controlled, *in vitro* experiment. The experiment used grip-to-grip measurements to estimate strain in excised porcine flexor tendons. Our objective is to demonstrate the acoustoelastic effect and its potential for biomechanical evaluation. The reported correlation coefficients should be considered specific to this experiment.

The nearly linear relationship between echo intensity and strain is further demonstrated as the linear approximation of strain based on echo, ε_{echo}, is statistically as capable of fitting the strain data points as a curve fit of the strain data, ε_{MTS}. This approximation was constructed using the curve fit of the echo intensity data, and thus is dependent on both echo intensity and stress data as input. However, knowing that there is a linear relationship between echo intensity and strain allows for calculations based solely on echo intensity data. In this example, strain can be approximated by dividing the echo intensity change by three. The next step will be to investigate other tissues *in vitro* and ultimately *in vivo*, to determine whether this relationship is always the same.

The nonlinear relationship between echo intensity and stress is exhibited by the logarithmic curve fit. Calculation of the nonlinear relationship allows for prediction of stress based solely on echo intensity (σ_{echo}). The relationship between strain and stress is also nonlinear, and was used to create a prediction of stress based on strain (σ_{ε}). Echo intensity was found to predict stress as well as a direct measurement of strain, provided the nonlinearity is anticipated and properly taken into account. The successful prediction of stress with echo intensity data allows for measurement of stress in a tissue based solely on echo intensity, rather than calculating strain and relating it to stress via a series of assumptions. Once translated to *in vivo* studies, this method can be used to gather information directly from living tissue on an individual basis. This allows for direct collection of mechanical data relevant to the study of interest. Rather than using cadaveric tissue, which is generally elderly, or donor tissue, which is often from pathologic sites, it would be possible to gather information from healthy, normal tissue in a relevant age range when conducting studies. Also, it allows taking data directly from tissues with the pathology of interest, rather than creating an animal model which may have inherent property differences and often do not correctly mimic the pathology. Because this method is noninvasive, pathologies and healing can be tracked over time.

The current study examined healthy flexor tendons at steady state conditions *in vitro*. To fully examine the relationship between

echo intensity and tissue stress and strain, it will be necessary to investigate the history- and time-dependent behaviors. Also, it will be important to study tissues in controlled loading settings *in vivo* to determine whether relationships between echo intensity and loading change in the tissue's native configuration. Finally, it will be important to study pathologic tissue. It has been reported that the mean echogenicity decreases in pathologic or damaged tissue (Crevier-Denoix et al., 2005), and it remains to be explored if this is proportional to the changes in mechanical properties.

In conclusion, echo intensity as defined herein is related linearly with strain, and nonlinearly with stress in porcine digital flexor tendons *in vitro*. By anticipating these relationships, we can predict stress and strain directly from ultrasonic echo intensity. This simple concept transforms standard clinical ultrasound systems into mechanical testing systems. Thus, it is possible to gather information about the stress–strain state of a tissue noninvasively, which is the first step towards *in vivo* evaluations of human tendons and other acoustoelastic tissues.

Conflict of interest statement

Two authors (RV and HK) hold a patent associated with some aspects of this concept for ultrasound analysis. No other authors have any conflicts of interest with the present study.

Acknowledgements

Support by the National Science Foundation (award 0553016) and National Institutes of Health (award R21 EB 008548) is gratefully acknowledged.

References

Abrahams, M., 1967. Mechanical behaviour of tendon in vitro. Medical and Biological Engineering and Computing 5, 433–443.

Anandan, P., 1989. A computational framework and an algorithm for the measurement of visual motion. International Journal of Computer Vision 2, 283–310.

Barron, J.L., Fleet, D.J., Beauchemin, S., 1994. Performance of optical flow techniques. International Journal of Computer Vision 12, 43–77.

Cohen, R.E., Hooley, C.J., McCrum, N.G., 1976. Viscoelastic creep of collagenous tissue. Journal of Biomechanics 9, 175–184.

Crevier-Denoix, N., Ruel, Y., Dardillat, C., Jerbi, H., Sanaa, M., Collober-Laugier, C., Ribot, X., Denoix, J.M., Pourcelot, P., 2005. Correlations between mean echogenicity and material properties of normal and diseased equine superficial digital flexor tendons: an in vitro segmental approach. Journal of Biomechanics 38, 2212–2220.

De Zordo, T., Lill, S.R., Fink, C., Feuchtner, G.M., Jaschke, W., Bellman-Weiler, R., Klauser, A.S., 2009. Real-time sonoelastography of lateral epicondylitis: comparison of findings between patients and healthy volunteers. American Journal of Roentgenology 193 (1), 180–185.

Doyley, M.M., Meaney, P.M., Bamber, J.C., 2000. Evaluation of an interactive reconstruction method for quantitative elastography. Physics in Medicine and Biology 45, 1521–1540.

Duan, Q., Angelini, E.D., Hertz, S.L., Ingrassia, C.M., Costa, K.D., Holmes, J.W., Homma, S., Laine, A.F., 2009. Region-based endocardium tracking on real-time three dimensional ultrasound. Ultrasound in Medicine and Biology 35 (2), 256–265.

Hughes, D.S., Kelly, J.L., 1953. Second-order elastic deformation of solids. Physics Review 92, 1145–1149.

Itoh, A., Ueno, E., Tohno, E., Kamma, H., Takahashi, H., Shiina, T., Yamakawa, M., Matsumura, T., 2006. Breast disease: clinical application of US elastography for diagnosis. Radiology 239, 341–350.

Kallel, F., Bertrand, M., 1996. Tissue elasticity reconstruction using linear perturbation method. IEEE Transactions on Medical Imaging 15 (3), 299–313.

Kallel, F., Bertrand, M., Ophir, J., 1996. Fundamental limitations on the contrast-transfer-efficiency in elastography: an analytic study. Ultrasound in Medicine and Biology 22, 463–470.

Ker, R.F., 2007. Mechanics of tendon from an engineering perspective. International Journal of Fatigue 29, 1001–1009.

Ker, R.F., Bennet, M.B., Bibby, S.R., Kester, R.C., Alexander, R.M., 1987. The spring in the arch of the human foot. Nature 325 (8), 147–149.

Kobayashi, H., Vanderby, R., 2005. New strain energy function for acoustoelastic analysis of dilatational waves in nearly incompressible, hyper-elastic materials. Journal of Applied Mechanics 72, 843–851.

Kobayashi, H., Vanderby, R., 2007. Acoustoelastic analysis of reflected waves in nearly incompressible, hyper-elastic materials: forward and inverse problems. Journal of the Acoustical Society of America 121 (2), 879–887.

Lloyd, D.G., Besier, T.F., 2003. An EMG-driven musculoskeletal model to estimate muscle forces and knee joint moments in vivo. Journal of Biomechanics 36, 765–776.

Maganaris, C.N., Paul, J.P., 1999. In vivo human tendon mechanical properties. Journal of Physiology 521 (1), 307–313.

Maganaris, C.N., Paul, J.P., 2000. Load-elongation characteristics of in vivo human tendon and aponeurosis. Journal of Experimental Biology 203, 751–756.

Ophir, J., Cespedes, E.I., Ponnekanti, H., Yazdi, Y., Li, X., 1991. Elastography: a quantitative method for imaging the elasticity of biological tissues. Ultrasonic Imaging 13, 111–133.

Pan, L., Zan, L., Foster, F.S., 1998. Ultrasonic and viscoelastic properties of skin under transverse mechanical stress in vitro. Ultrasound in Medicine and Biology 24 (7), 995–1007.

Ponnekanti, H., Ophir, J., Cespedes, I., 1992. Axial stress distributions between coaxial compressors in elastography: an analytical model. Ultrasound in Medicine and Biology 18, 667–673.

Ponnekanti, H., Ophir, J., Huang, Y., Cespedes, I., 1995. Fundamental mechanical limitations on the visualization of elasticity contrast in elastography. Ultrasound in Medicine and Biology 21, 533–543.

Riemersma, D.J., Schamhardt, H.C., Hartman, W., Lammertink, J.L.M.A., 1988. Kinetics and kinematics of the equine hind limb: in vivo tendon loads and force plate measurements in ponies. American Journal of Veterinary Research 49 (8), 1344–1352.

Rigby, B.J., Hirai, N., Spikes, J.D., Eyring, H., 1959. The mechanical properties of rat tail tendon. Journal of General Physiology 43, 265–283.

Samani, A., Zubovits, J., Plewes, D., 2007. Elastic moduli of normal and pathologic breast tissues: an inversion-technique-based investigation of 169 samples. Physics in Medicine and Biology 52 (6), 1565–1576.

Skovorada, A.R., Emelianov, S.Y., Lubinsky, M.A., Sarvazyan, A.P., O'Donnel, M., 1994. Theoretical analysis and verification of ultrasound displacement and strain imaging. IEEE Transactions on Ultrasonics, Ferroelectrics and Frequency Control 41 (3), 302–313.

Skovorada, A.R., Emelianov, S.Y., O'Donnel, M., 1995. Tissue elasticity reconstruction based on ultrasonic displacement and strain images. IEEE Transactions on Ultrasonics, Ferroelectrics and Frequency Control 42 (4), 747–765.

Woo, S.L.-Y., Gomez, M.A., Woo, Y.-K., Akeson, W.Y., 1982. Mechanical properties of tendons and ligaments I: quasi-static and nonlinear viscoelastic properties. Biorheology 19, 385–396.

Zhi, H., Ou, B., Luo, B.M., Feng, X., Wen, Y.L., Yang, H.Y., 2007. Comparison of ultrasound elastography mammography and sonography in the diagnosis of solid breast lesions. Journal of Ultrasound in Medicine 26, 807–815.